Periodicals of Engineering and Natural Sciences ISSN 2303-4521
Vol. 9, No. 1, February 2021, pp.346-360

Fabrication of ZnO/nanobentonite as a new efficient adsorbent for rapid elimination of xylenol orange dye

Ahmed Abbas Obaid [1], Husham Mohammed Al.Tameemi [2], Kassim Kadhim Hameed [3]
[1,2,3] Department of Chemical Engineering,University of Al-Qadisiyah

ABSTRACT

A novel ZnO-nanobentonite (ZnO/NB) nanocomposite was successfully prepared using hexadecyltrimethylammonium bromide (HDTMA) as a surfactant and used as an efficient adsorbent to remove the xylenol orange (XO) from aqueous solutions. The fabricated nanocomposite was fully characterized by FTIR, FESEM, XRD, EDX, and BET measurements. The ZnO33%/NB sample with a high SBET and low total pore volume compared with the nanobentonite clay, based on BET results, indicated an increase in SBET due to the incorporation of ZnO nanoparticles into the layer of nanobentonite. For achieving the optimum condition, the effect of ZnO33%/NB sorbent dosage, initial pH, reaction time, and primary dye concentration, on XO dye elimination was investigated. The result show that the 97% elimination of XO dye occurred at optimum condition (40 mgl/l of dye concentration, pH 2, 15 mg of ZnO33%/NB adsorbent at 30 minutes), and the adsorption capacity and residual XO after treatment at these conditions is 48.5 and 1.2 ppm, respectively. Langmuir models and Freundlich model were used to studying the adsorption isotherms of the elimination process and results authenticated that XO dye adsorption followed the Langmuir model. Also, the recycling experiments showed that ZnO33%/NB adsorbent had more stability and recoverability. High adsorption capacity, simple fabrication method, short reaction time, and supreme reusability of ZnO33%/NB nanocomposite make it an effective sorbent for the elimination of XO dye from wastewaters.

Keywords: Xylenol Orange; rapid elimination; Adsorption isotherms; Nano-composite; Langmuir model; Freundlich model.

Corresponding Author:

Ahmed Abbas Obaid
Department of Chemical Engineering,
University of Al-Qadisiyah, Iraq
E-mail: ahmed.ubeed@qu.edu.iq

1. Introduction

Today, water effluent with diverse pollutants is a significant environmental challenge [1]. Organic dyes one of the main water pollutants that are extensively distributed in the environment via wastewater discharged from textile, rubber, pharmaceutical, plastic leather, paper, and painting industries, it causes widely environmental damages and these dyes lead to effect harmful to individuals and the whole types of life [2-4]. Xylenol orange (XO) is an organic dye reagent with a triphenylmethane structure, most widely utilized as a chemical indicator for the determination of many heavy metals due it is superior potentiometric reagent and complexometric indicator[5]. It is used in several processes of textile industries and laboratories. Xylenol orange is toxic both for aquatic animals and human beings because the presence of XO in the wastewater more absorbs heavy metals with complex formation [5-7]. Also, XO in water bodies can intermeddle with the growth of bacteria [8]. Accordingly, it is urgent to find an ideal technique for removing this dye from wastewaters. Until now, different Chemical, physical and biological procedures were applied for treating the water pollutants, such as solvent extraction, biological treatments, membrane filtration, chemical coagulation/flocculation, electrolysis, photo-degradation, reverse osmosis, and adsorption process [9-14]. Among them, the adsorption method is considered the most popular, easy, environmentally friendly, economical, effective, adaptable, and simple-workup to remove organic dyes from aquatic media [15-18]. Nowadays, the adsorption procedures are broadly utilized for

removing diverse pollutants from wastewater [19]. However, finding a highly efficient sorbent is one of the main serious parameters of the used application of the adsorption process.

Clays are prevalent, low-cost, and easily available chemical compounds that belong to a broader group of minerals [20]. Bentonite is a natural clay mineral composed of rich concentrations of Na^+, Li^+, and Ca^{2+} ions located among layers of silicon ions [21, 22]. The structural characteristic of bentonite can be applied as supports for the deposition of deferent catalysts or can be modified via diverse procedures. The utilization of catalytic support goals to modify the scattering of the active phase and enhance the surface area leading to high active sites [23, 24].

The Bentonite has many merits, make it a good choice for using it as a support, such as good adsorption performance, large specific surface area, low cost, high stabilization, and high ion exchange capacity [25, 26].

ZnO is a non-toxic, low-cost, safely, and easily available catalyst, which has got great interest in various organic reactions [27-29], and absorption process [30-32]. To improve the adsorption process, the incorporation of metal oxide on a porous material like bentonite is a successful procedure. To date, many papers have been published on the use of modified bentonite and bentonite as an absorbent to remove pollutants from industrial wastewater. such as Fe3O4-chitosan@bentonite for the elimination of heavy metals [33], Mn2+-modified bentonite for the elimination of Fluoride [34], bentonite@MnFe2O4 composite for the removal of Cr (III) [35], organo-modified bentonite (CTAB-B) for the elimination of Congo red dye [36], activated bentonite-alginate composite for the elimination of methylene blue dye [37] and TiO2-bentonite for the removal of methylene blue dye under UV light [38].

This paper introduced a little modified procedure to increase the amount loading of zinc oxide nanoparticles on nanobentonite in ZnO/nanobentonite via by modifying nano-bentonite with hexadecyltrimethylammonium as a surfactant, before adding ZnCl2 solution.

The adsorption of XO organic dye onto ZnO/NB nanocomposite and the effects of the parameters (the primary XO concentration, adsorbent dose, contact time, and pH) on the adsorption process were investigated.

2. Material and methods

2.1 Materials

Each of the materials and reagents was provided by Fluka and Merck. The clay used is hydrophilic nanobentonite obtained from Sigma-Aldrich. The patterns of XRD were recorded via the radiation of CuKα at 30 mA, 40 keV, and 3º min-1 scanning rate using X'Pert MPD diffractometer. FTIR spectra were recorded by an 8400 Shimadzu Fourier transform spectrophotometer with KBr pellets. FE-SEM images were taken by HITACHI S-4160 instrument type to study particle distribution and morphology. The total surface area of the samples was determined by N2 adsorption at the temperature of liquid nitrogen with Belsorp II (BEL Japan, Inc.). The Inductively Coupled Plasma (ICP-OES) was used for measuring the zinc amount in each prepared sample on a Varian Australia, Vista-pro model. UV-vis Data were obtained by using a Carry 100 Conc Varian spectrophotometer.

2.2 Fabrication of ZnO/NB nanocomposite by HDTMA

The samples of ZnO/NB were prepared by the in-situ synthesis of Zn (zinc oxide) on the surface of nano bentonite for immobilized it. ZnCl2 with 0.3 M concentration was prepared in 25 ml deionized water with half an hour of stirring. Hydroxide sodium (NaOH) solution (4M) was added drop by drop to this solution to make the pH of the solution equal 12, then a continuous stirring was applied for 6 hours at 75 °C. Meanwhile, one-gram nanobentonite was diffused in 15 ml of HDTMA solution (hexadecyltrimethylammonium solution (0.1M)) and then stirred for one day at 75 ºC to obtain HDTMA/NB sample. Thereafter, the NaOH solution and aqueous solution of zinc chloride mixture was added drop-wise into HDTMA/NB suspension with steady stirring for 20 h at 75 ºC. The resulting solid product was filtrated for separating it from the solution, then it was washed more than one time via deionized H2O, and it was dried for 48 h at 80 ºC. Ultimately, the fabricated precipitate was calcined for 6 h in a furnace at 500 ºC for preparing nanocomposite of ZnO33%/NB [39].

2.3 Fabrication of ZnO/NB nanocomposite in the absence of HDTMA

In this procedure, Zn/BN was primarily obtained via adding one-gram nanobentonite into 20 ml of 0.3 M ZnCl2 solution, this suspension (mixture) was heated for 20 h at 75 ºC. Afterward, Zn/NB sample was filtrated, washed

a few times with deionized water, then was dried for 48 hours at temperature 80 ºC. The product of the fabricated precipitate was heated at 500 ºC for 6 h in a furnace for calcination it and to make ZnO5%/NB nanocomposite.

2.4 Investigation of the Efficiency of ZnO33%/NB nanocomposite

To accomplish the elimination of xylenol orange dye from contaminant water the following procedures are followed. First UV-vis at 436 nanometers was used for the determination of the dye concentration. Then the adsorption test analyses were performed by equilibrating 15 mg of the ZnO33%/NB via 50 ml of the XO solution with the desired concentration (10–120 ppm) at a pH value of (2-10) for the required time. After complete reaction, the mixture (suspension) was centrifuged, then the concentration of XO dye which was adsorbed by the ZnO33%/NB nanocomposite was determined by spectrophotometry at the wavelength (λ) equal to 436 nm. The value of qe (mg/g) (the equilibrium capacity adsorption) and (R%) (rate of removal) were calculated by the below equations [40]:

(Eq. 1) $qe=\frac{(C0-Ce).V}{M}$

(Eq. 2) $R\% = \frac{(C0-Ce)100}{Co}$

Wherein Ce and C0 are the final and initial concentrations of the XO dye (mg lit-1), M (g) is the volume of XO dye solution and the weight of ZnO33%/NB adsorbent, respectively. And V is the sample volume in Liters.

3. Results and discussion

3.1 Characterization of ZnO/NB nanocomposite with ICP-OES analysis

The content of Zn in the ZnO/NB nanocomposite was determined by ICP-OES., 4 ml of concentrated HClO4: HNO3 (1:1) was added to a precise content of the ZnO/NB and warmed at 120 ºC to dry it. This was repeated 4 times after that 4 ml of Hydrofluoric acid was poured and warmed at 120 ºC to destroy the clay structure. Next, 15 ml of dilute HCl was poured and the mixture was warmed for half an hour. The resultant solution was applied for the determination of Zn, after filtration and dilution in a flask of 50 ml [39]. The amounts of zinc oxide in the fabricated ZnO/NB without and mediated with HDTMA were 5 and 33%, respectively, as measured by ICP-OES analysis. These results showed that the ZnO amount on ZnO/NB nanocomposite was remarkably increased in the presence of HDTMA surfactant. These results could probably be described by considering increased interactions of the anionic precursor with HDTMA modifier.

3.2 Analysis by FTIR

Figure 1 shows the FT-IR spectra of nanobentonite, HDTMA/NB, and ZnO33%/NB nanocomposite. In Figure 1a the Si–O bending and O-H stretching vibrations are observed at 1025 and 3623 cm−1, individually. The bands at 520 and 753 cm−1 cans be related to symmetric vibrations of Si–O–Al, and the bands at 836 and 913 cm−1 related to bending vibrations of Al-Mg–OH. In the spectrum of HDTMA/NB (Figure 1b), two novel peaks around 2852 and 2921 cm-1, connected with the stretching vibrations of C-H in the hydrocarbon chains, were observed which are related to the HDTMA surfactant molecules. In Figure 1c, the weak bands situated around 400-600 cm−1 correspond to the zinc oxide stretching vibrations, which have been demonstrated for zinc oxide in diverse nanocomposites. Generally, in the infrared spectrum of zinc oxide, the three peaks situated at 527, 454, and 425 cm−1 are linked to the Zn-O vibrations [39, 41]. These bands were weakly in ZnO33%/NB, because of the confined ion exchange capacity of nanobentonite to receive Zn2+ ions; thus, they overlapped with bands relating to the vibration modes. The same results were observed in the literature [39].

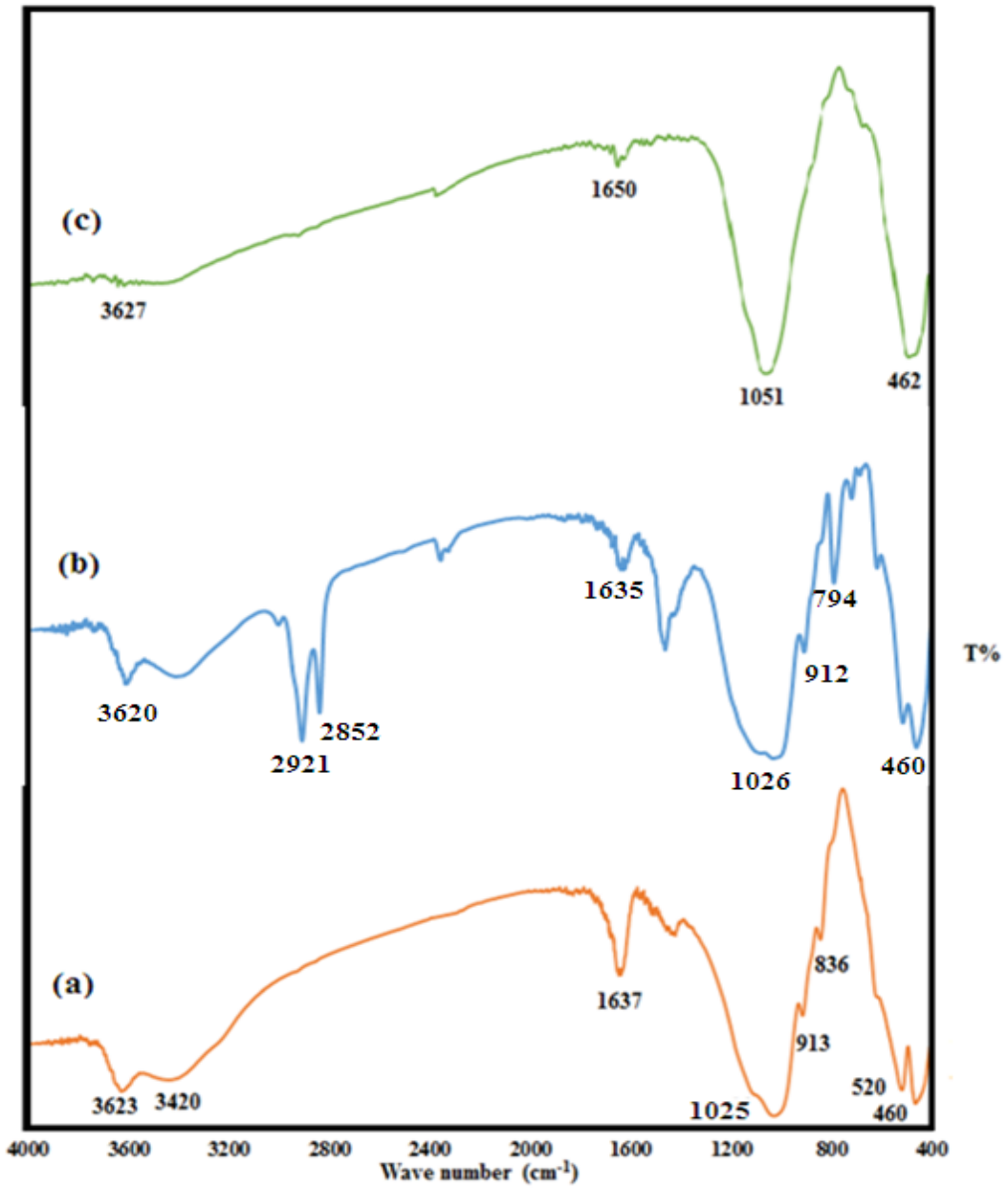

Figure 1. FTIR spectra of (a) nanobentonite, (b) HDTMA/NB, and (c) ZnO33%/NB nanocomposite.

3.3 XRD investigations

To investigate the phase and structure of the crystalline of the nanobentonite clay and prepared ZnO33%/NB nanocomposite the XRD analysis was recorded at room temperature as demonstrated in Figure 2. The characteristic peaks at 2θ values in 7.2, 19.9, 34.8, and 63.9º in Figure 2a agreement with the crystalline structure of montmorillonite [42, 43] which authenticated that the applied nanobentonite has a montmorillonite structure as the main phase. Also, the nanobentonite exhibited an intense and main diffraction line with a d–value of 1.25 nm at a 2θ of 7.2º value, identical to the reflection d001, which shifted to 2θ= 9.06º with a d–value of 0.974 nm In the ZnO33%/NB nanocomposite [42]. The decrease of 0.276 nm in the space among the layers of nanobentonite could be related to the loading of Zinc oxide nanoparticles on the surface of nanobentonite layers. A comparison of the XRD spectra of nanobentonite and ZnO33%/NB nanocomposite demonstrated that the

framework of nanobentonite remains undamaged following calcination processes and ion exchange. The Scherrer equation was used to measure the particle size of the ZnO33%/NB (Eq. 3).

$$D=0.94\lambda/\beta D \cos\theta \quad \text{(Eq. 3)}$$

Where λ is the radiation wavelength (for Cu-Kα radiation is 1.54056 Aº), D is the particle size (nm), βD is the width of the peak at the half-maximum intensity, and θ is the position of peak [44].
By this equation, the average crystallite sizes of ZnO33%/NB nanocomposite were computed 26.5 nm.

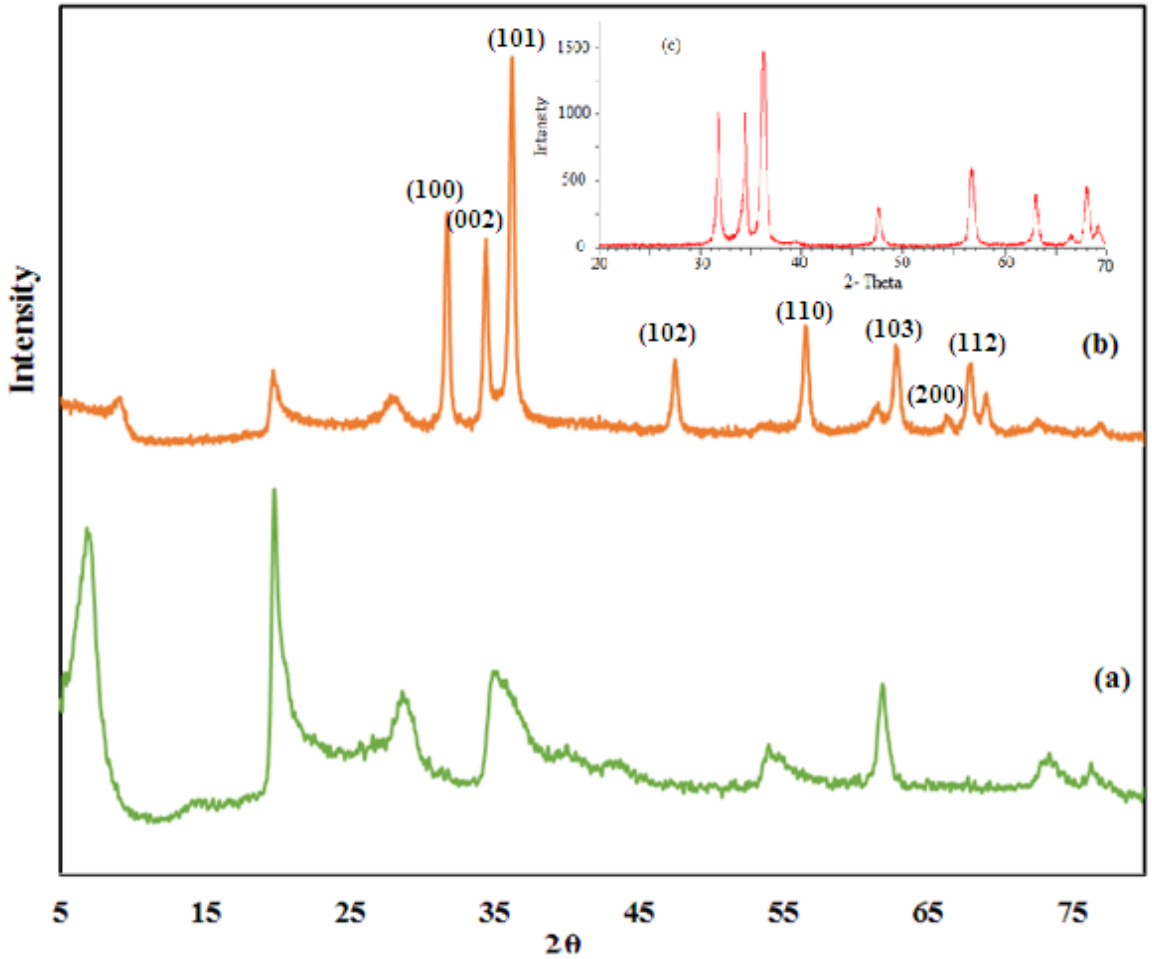

Figure 2. XRD spectra of nanobentonite (a), ZnO33%/NB nanocomposite (b), and ZnO nanoparticle (insert c). Pattern (c) is reproduced from Tayebee et al [29].

3.4 EDX and FESEM results

The morphology of the surface of nanobentonite clay and ZnO33%/NB were investigated by FESEM analyses as shown in Figure 3. The comparison of FESEM images of nanobentonite (Figure 3a, b) and ZnO33%/NB nanocomposite (Figure 3c, d) proved the prosperous immobilization of zinc oxide particles on the surface of nanobentonite clay. Based on FESEM photos of the ZnO33%/NB sample, it appears to be that the interlayer spaces and pores of nanobentonite were decreased via ZnO, and the porosity of the ZnO33%/NB is diminished. Also, the mean particle sizes of the prepared sample would be ~32 nm.

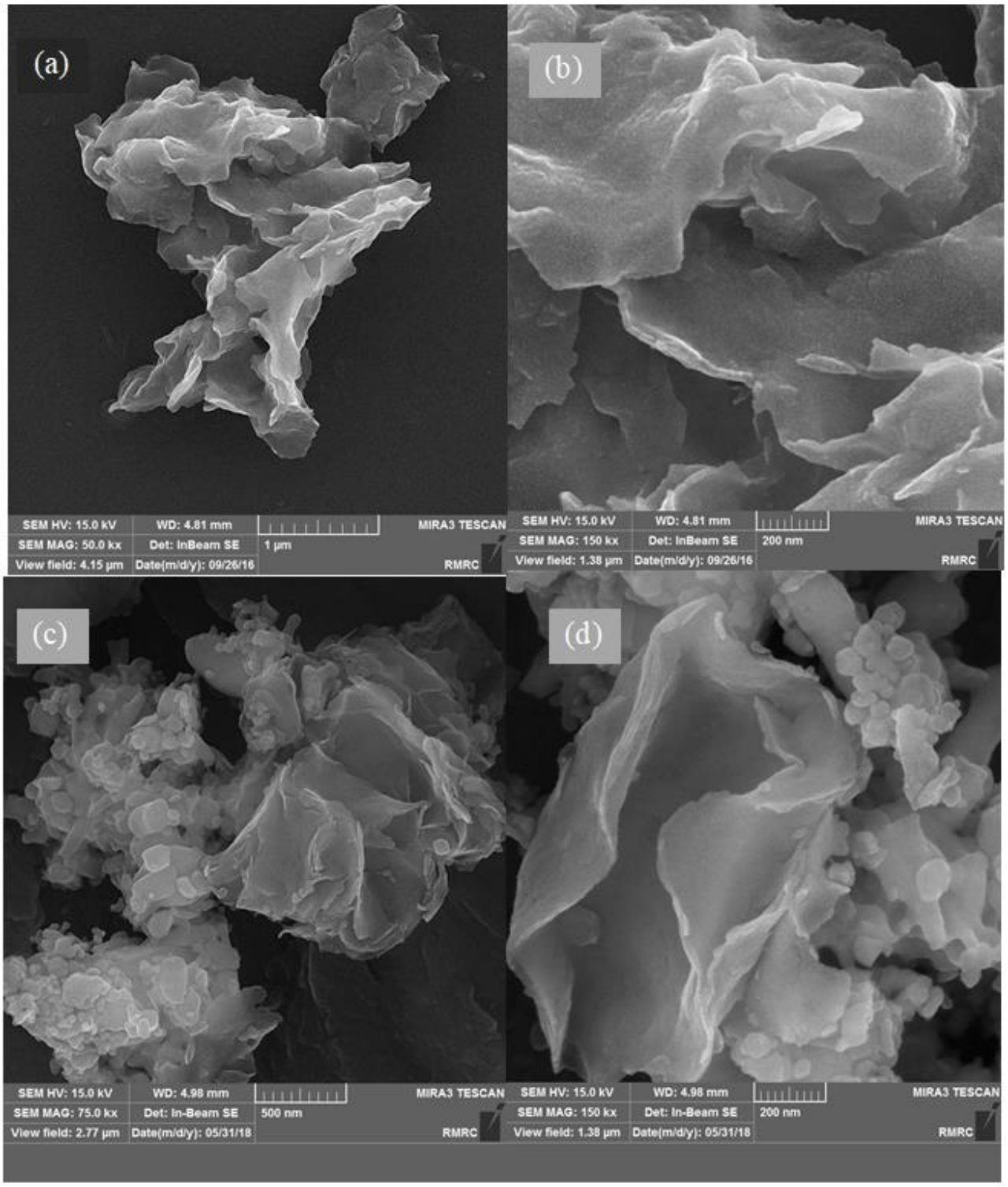

Figure 3. FESEM images of nanobentonite (a, b) and $ZnO_{33\%}$/NB nanocomposite (c, d).

The EDX experiment of the nanobentonite and ZnO33%/NB was shown in Figure 4. Figure 4b showed the presence of Zn, Al, Mg, O, K, Fe, Ca, and Si in the prepared ZnO33%/NB sample and affirmed that ZnO has comprised onto the clay framework in the samples of the nanocomposite.

The EDX spectrum of Zn characteristic has lines situated in 9.6, 8.6, and 1.0 keV of ZnO33%/NB, where best agreement with the literature was achieved [40, 45].

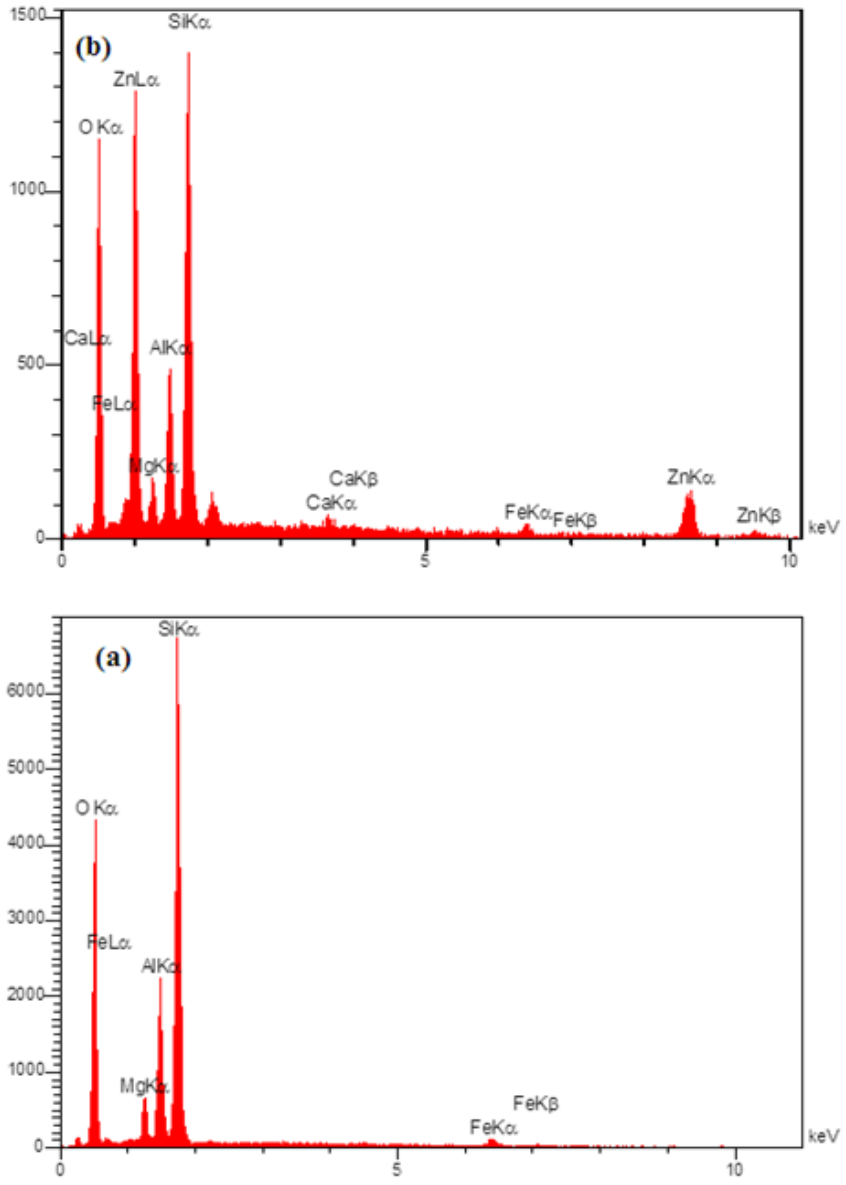

Figure 4. EDX analysis of nanobentonite (a) and ZnO33%/NB nanocomposite (b).

3.5 BET investigation

The surface texture characterization of nanobentonite and ZnO33%/NB nanocomposite was investigated through BET analysis Table 1.

According to the results, the sample surface area was increased after the immobilization of zinc oxide in the nanobentonite structure, while the total pore volume was diminished.

Table 1. Pore volume and Surface area of nanobentonite and ZnO33%/NB nanocomposite

Clay	Surface area (m2g-1)	Total pore volume (cm3g-1)
Nanobentonite	63	0.462
ZnO/nanobentonite	126.584	0.384

3.6 Adsorption experiment

3.6.1 The effect of sorbent dose

To optimize the primary sorbent dose, a series of experiments were done by the sorbent amount of ZnO33%/NB (5, 10, 15, 20, 25, and 30 mgl-1) at pH 2 in 50 ml of 40 ppm XO solutions (Figure 5). The Results demonstrated that only a trace amount (~6%) of XO dye was eliminated and 37.6 ppm of XO remained in the absorbent-free condition after 30 min; while in the presence of 5 mgl/l of the ZnO33%/NB adsorbent, removal% was expanded from 6 to 53. The increasing amount of the adsorbent improved the removal% in the account of enhance in the number of active sites. Even though, more increase in the adsorbent amount from 15 to 30 mgl/l, led to reducing removal%, from 97 to 87. This outcome would be elucidated concerning agglomeration of the adsorbent active sites by enhancing the adsorbent dose, resulted in a reducing concentration of the XO dye at the active sites and diminishing removal%. Therefore, 15 mgl/l of the ZnO33%/NB adsorbent was enough to achieve the maximum removal%.

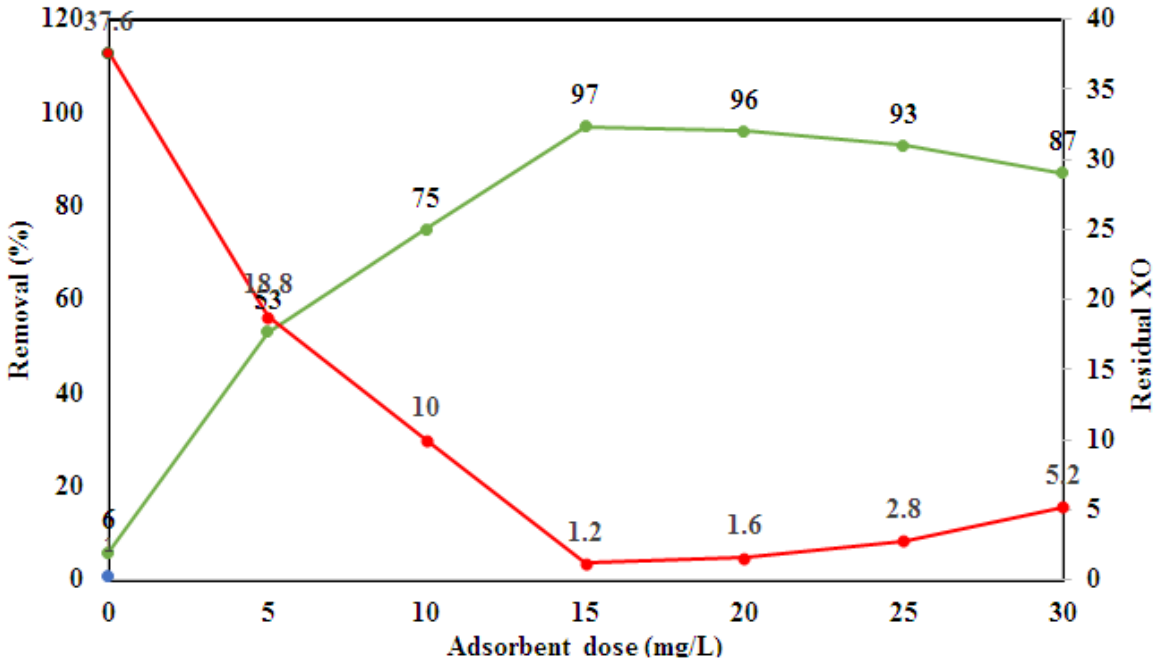

Figure 5. The elimination and residual of XO dye relation with adsorbent dosage of ZnO33%/NB

3.6.2 The effect of pH

The effect of initial pH in the adsorption of XO dye was performed in the range of 2 to 10 with 15 mgl-1 of adsorbent dosage, at the constant primary concentration of 40 ppm of XO within 30 min (Figure 6). Based on Figure 5 the ZnO33%/NB nanocomposite adsorbed a high quantity of XO (97%) at low (acidic) pH 2, but, the adsorption of XO dye was diminished with an increase in pH. According to the literature, in an aqueous solution, the acidic dye is initially dissolved and next dissociate and as a result, anionic dye ions are comprised, also, at low pH, positive charge sites formed on the adsorbent surface [46-49]. So, it produces a remarkably most electrostatic attraction among the anionic dye and the positively charged surface of the ZnO33%/NB adsorbent. However, as the pH increased, the amount of negatively charged sites of XO dye enhanced and the amount of positively charged sites of adsorbent diminished. As a result, the electrostatic repulsion between negative surface sites of the nanocomposite adsorbent and dye anions in high pH did not favorable for more adsorption of XO dye. Therefore, the pH of 2 was chosen as an optimum pH to achieve high removal of XO dye from aqueous solutions.

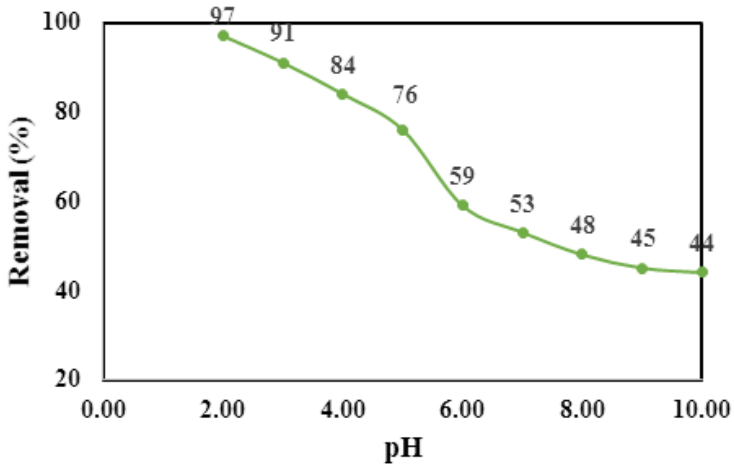

Figure 6. The adsorption of xylenol orange onto ZnO33%/NB nanocomposite at various pH

3.6.3 The effect of initial dye concentration

The effect of concentration of the dye has a distinguished role in the amount of adsorbed dye and the performance of the removal of the dye. Commonly, increasing the initial concentration of the dye causes a reducing percentage of dye removal which is due to the saturation of adsorption sites over the absorbing surface [50, 51]. The effect of the diverse primary concentrations (10, 20, 40, 60, 80, 100, and 120 ppm) of XO on the adsorption onto the surface ZnO33%/NB under the conditions the 15mgl-1 adsorbent dosage, pH 2, and 25 °C was investigated (Figure 7). The results show that with an increase in the initial concentration of the dye, the dye elimination diminishes. The reason for this phenomenon is that with increasing the XO concentration the active surface of the ZnO33%/NB composite decreased. The adsorption system is extremely dependent on the primary concentration of the dye solution. So, the final concentration of 40 ppm was selected to achieve the maximum removal of XO dye.

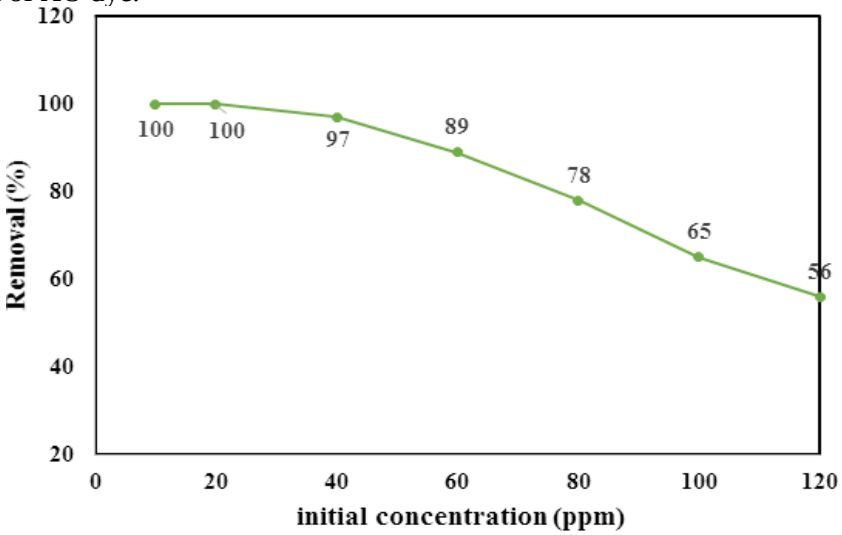

Figure 7. Influence of initial XO dye concentration on the elimination of XO dye.

3.6.4. The effect of adsorption contact time

To the sufficient removal of the dyes from diverse sources, the adsorption contact time should be short sufficient for the time using in the industrial applications and the experiments in the laboratories [48]. The removal of XO dye by ZnO33%/NB adsorbent at various adsorption contact times in the optimum condition is shown in Figure 8. The results show that the removal of the XO dye molecules was increased as enhanced the adsorption contact time and then almost fixed after 30 min. Also, the rate of XO removal was fast, initially, and then slow down gradually until it achieved the equilibrium, and further on there was no considerable enhance of dye removal.

This might be because of the saturation of active surface sites of the ZnO33%/NB adsorbents. Therefore, 30 min was chosen as an optimum adsorption contact time to achieve the maximum removal of XO dye.

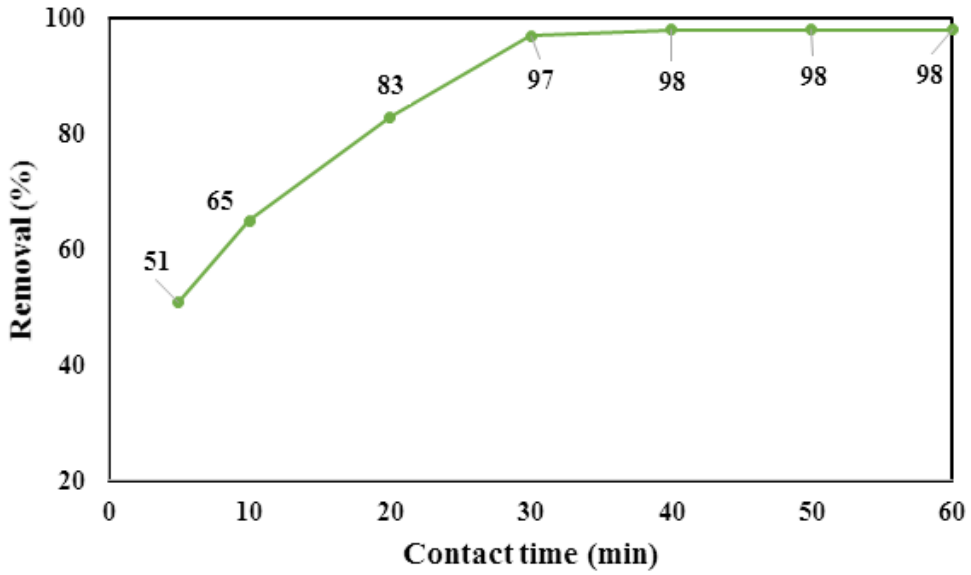

Figure 8. The removal of xylenol orange from aqueous solution by ZnO33%/NB, as a function of contact time

3.7 Adsorption isotherms

Investigation Xylenol orange adsorption using Langmuir and Freundlich adsorption isotherm models is accomplished with initial concentrations (10-120 ppm) onto ZnO33%/NB adsorbent at pH 2 and it was demonstrated in Figure 9a. The Langmuir model assumed at specific homogeneous sites, over the adsorbing surface that the adsorption takes place in monolayer form, and is formulated in linear form as follows [52- 54]:

(Eq. 4) $$\frac{Ce}{qe} = \frac{Ce}{qm} + \frac{1}{qm\,kL}$$

Where Ce, qm, KL, and are the equilibrium concentration of contaminant solution (mg l-1), the high adsorption capacity (mg g-1), and the Langmuir constant (mg l-1), respectively, that qm and KL were accounted from the slope and intercept of isotherm diagrams (see Table. 2). The maximum adsorption capacity of XO dye by ZnO33%/NB adsorbent was 11.95 mg g-1, confirming that the ZnO33%/NB composite demonstrated supreme adsorption capacities for XO dye. The RL parameter which it is give the best prediction to the desirability of the adsorption process has been offered as follows [55]:

(Eq. 5) $$R_L = \frac{1}{1+K_L C_o}$$

Where the RL value determines the type of the isotherm model. The RL factor values (0-1) demonstrated that the adsorption of chosen XO dye into the ZnO33%/NB adsorbent was desirable (Table 2).

The Freundlich equation was studied to fit the data of XO dye adsorption isotherms through follows the equation [56-59]:

(Eq. 6) $$Logqe = Logkf + \frac{1}{n}.LogCe$$

Where Kf (mgg-1) and n illustrate Freundlich constant and heterogeneity parameter. The Freundlich isotherm of XO dye is depicted in (Figure 9b). As shown in Table 2 and according to values of the R2, the adsorption fitted the Langmuir model more than the Freundlich model.

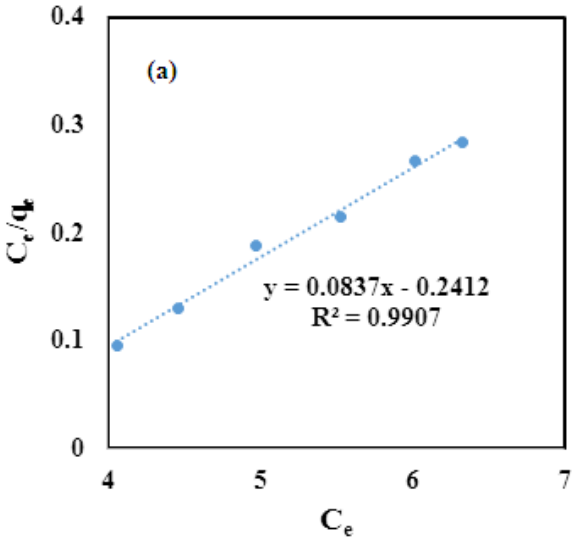

Figure 9. (a) Adsorption isotherm of Langmuir

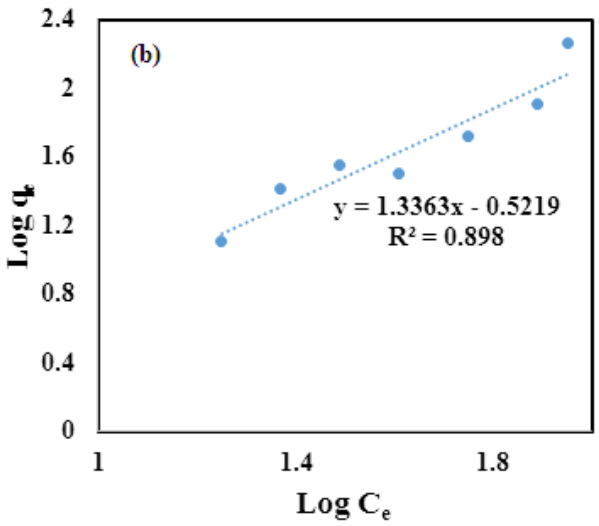

Figure 9. (b) Adsorption isotherm of Freundlich

Table 2. The Langmuir and Freundlich isotherm parameters for the adsorption of XO dye by ZnO33%/NB composite

	Langmuir				Freundlich		
Dye	qm (mg/g)	KL (L/mg)	R2	RL	Kf (mg/g)	n	R2
XO	11.95	0.347	0.9907	0.002-0.365	3.33	0.750	0.898

3.8 Recyclability and stability of the ZnO33%/NB nanocomposite adsorbent

The investigation of the ZnO33%/NB reusability was carried out by cycle of experiments by using a mixture of deionized water, NaCl (0.5 M), and hot ethanol as solvent. For this goal, the ZnO33%/NB composite was thoroughly separated via simple filtration and washed with desorption solvents, and then washed 4 times with deionized water and then dried at 100 °C for 8 h. The recovered ZnO33%/NB was tested its ability for adsorption by reusing it in the adsorption process under constant conditions.

The findings demonstrate that the ZnO33%/NB nanocomposite is reusable for at least five cycles without a remarkable loss of activity (Figure10).

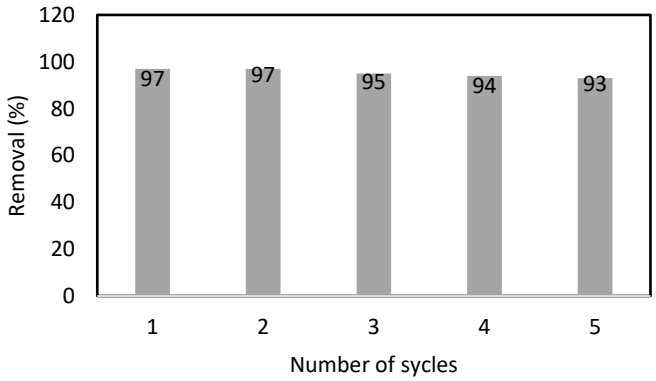

Figure 10. Reusability of the ZnO33%/NB nanocomposite in the elimination of XO dye

3.9. Comparison of adsorption capability of ZnO33%/NB nanocomposite with another adsorbent

The superiority of the ZnO33%/NB nanocomposite adsorbent in the removal of XO dye from aqueous solutions was checked by comparing the acquired outcomes with several adsorbents reported in the literature (Table 3).

According to table 3, it is clear that concerning the removal percentage, and adsorption time the present procedure is highly proper and superior.

Table 3. Comparison of the ZnO/NB nanocomposite in the removal of XO dye with several reported adsorbent

Adsorbent	**Time (min)**	**Removal (%)**	**Ref.**
Coal Ash	40	80	[48]
natural Bauxite (BXT)	120	75	[59]
HDTMA-BXT	30	98.6	[59]
Chitosan Microsphere	120	93.8	[60]
Molecularly Imprinting Polymers (MIP)	60	80	[5]
Fe3O4 + H2O2	45	94	[61]
MnO2	30	95	[62]
Nano ZnO	60	72	This work
Nanobentonite clay	60	52	This work
HDTMA/NB	60	77	This work
ZnO5%/NB	30	83	This work
ZnO33%/NB	30	97	This work

4. Conclusion

Bentonite clay has been famous as an inexpensive sorbent over the last few decades because of its native, modification capability, and plenty of availability. For the first time, this paper represents the fabrication of the ZnO/NB nanocomposite by applying HDTMA as a surfactant. The results demonstrated that the fabricated ZnO33%/NB sample mediated via HDTMA surfactant had high amounts of nanoparticles of ZnO on the surface of nanobentonite than the ZnO5%/NB fabricated without the mediation of HDTMA. The ZnO33%/NB in comparison with the nanobentonite clay, and ZnO nanoparticles, shows high adsorption capacity, short reaction time, and effective removal of XO dye from solutions. Influence parameters on the removal% such as sorbent dosage, initial pH, primary dye concentration, and a time reaction were checked and the findings demonstrated that the 97% elimination of XO dye occurred at 40 mgl-1 of dye concentration, pH 2, 15 mg of ZnO33%/NB adsorbent in during of 30 minutes. Moreover, the adsorption isotherms displayed that the adsorption process of XO dye follows Langmuir isotherm. The XO yield removal was 93 % after recycling the ZnO33%/NB sample for 5 runs. Therefore, the ZnO33%/NB nanocomposite can be applied as a promising sorbent for treating wastewater involving resistant organic dyes.

References

[1] C.R. Holkar, A.J. Jadhav, D.V. Pinjari, N.M. Mahamuni, A.B. Pandit, A critical review on textile wastewater treatments: Possible approaches, Journal of Environmental Management, 182 (2016) 351-366.

[2] V. Katheresan, J. Kansedo, S.Y. Lau, Efficiency of various recent wastewater dye removal methods: a review, Journal of environmental chemical engineering, 6 (2018) 4676-4697.

[3] S. Pai, M.S. Kini, R. Selvaraj, A review on adsorptive removal of dyes from wastewater by hydroxyapatite nanocomposites, Environmental Science and Pollution Research, (2019).

[4] J. Fan, D. Chen, N. Li, Q. Xu, H. Li, J. He, J. Lu, Adsorption and biodegradation of dye in wastewater with Fe3O4@ MIL-100 (Fe) core–shell bio-nanocomposites, Chemosphere, 191 (2018) 315-323.

[5] S.A. Bhawani, N.A.B. Daud, S. Bakhtiar, R.M. Roland, M.N.M. Ibrahim, Synthesis of Molecularly Imprinting Polymers for the Removal of Xylenol Orange from Water, Nature Environment and Pollution Technology, 19 (2020) 825-830.
[6] M. Garrudo-Guirado, A. Blanco-Flores, H. Toledo-Jaldin, V. Sánchez-Mendieta, A. Vilchis-Néstor, Reuse of sustainable materials for xylenol orange dye and copper (II) ion ammoniacal removal, Journal of environmental management, 206 (2018) 920-928.
[7] X. Pang, C. Yang, S. Ren, Adsorption capacity of expansion graphite for xylenol Orange, Journal of Materials Science and Chemical Engineering, 1 (2013) 1-5.
[8] X.L. Xiong, C.B. Shao, Removal of Xylenol Orange from Solutions by γ-Cyclodextrin-Grafted Carboxymethyl Cellulose, Advanced Materials Research, Trans Tech Publ, 2011, pp. 1180-1183.
[9] A. Hamedi, M.B. Zarandi, M.R. Nateghi, Highly efficient removal of dye pollutants by MIL-101 (Fe) metal-organic framework loaded magnetic particles mediated by Poly L-Dopa, Journal of Environmental Chemical Engineering, 7 (2019) 102882.
[10] G. Hitkari, S. Singh, G. Pandey, Synthesis, Characterization and Visible Light Degradation of Organic dye by Chemically Synthesized ZnO/ γ-Fe3O4 Nanocomposites, Synthesis, 4 (2017).
[11] F. Rahman, M. Akter, Removal of dyes form textile wastewater by adsorption using shrimp shell, Int J Waste Resour, 6 (2016) 2.
[12] D. Bhatia, N.R. Sharma, J. Singh, R.S. Kanwar, Biological methods for textile dye removal from wastewater: A review, Critical Reviews in Environmental Science and Technology, 47 (2017) 1836-1876.
[13] T.W. Seow, C.K. Lim, Removal of dye by adsorption: a review, International Journal of Applied Engineering Research, 11 (2016) 2675-2679.
[14] N.R.J. Hynes, J.S. Kumar, H. Kamyab, J.A.J. Sujana, O.A. Al-Khashman, Y. Kuslu, A. Ene, B. Suresh Kumar, Modern enabling techniques and adsorbents based dye removal with sustainability concerns in textile industrial sector -A comprehensive review, Journal of Cleaner Production, 272 (2020) 122636.
[15] S. Saber-Samandari, S. Saber-Samandari, H. Joneidi-Yekta, M. Mohseni, Adsorption of anionic and cationic dyes from aqueous solution using gelatin-based magnetic nanocomposite beads comprising carboxylic acid functionalized carbon nanotube, Chemical Engineering Journal, 308 (2017) 1133-1144.
[16] S. Guo, K. Wu, Y. Gao, L. Liu, X. Zhu, X. Li, F. Zhang, Efficient removal of Zn (II), Pb (II), and Cd (II) in waste water based on magnetic graphitic carbon nitride materials with enhanced adsorption capacity, Journal of Chemical & Engineering Data, 63 (2018) 3902-3912.
[17] A. Nasar, S. Shakoor, Remediation of dyes from industrial wastewater using low-cost adsorbents, Materials Research Foundations, 15 (2017).
[18] S. Mustapha, M. Ndamitso, A. Abdulkareem, J. Tijani, D. Shuaib, A. Ajala, A. Mohammed, Application of TiO 2 and ZnO nanoparticles immobilized on clay in wastewater treatment: a review, Applied Water Science, 10 (2020) 1-36.
[19] H. Abbasi, F. Salimi, F. Golmohammadi, Removal of Cadmium from Aqueous Solution by Nano Composites of Bentonite/TiO 2 and Bentonite/ZnO Using Photocatalysis Adsorption Process, Silicon, (2020) 1-11.
[20] G. Nagendrappa, Organic synthesis using clay and clay-supported catalysts, Applied Clay Science, 53 (2011) 106-138.
[21] M. Moosavi, Bentonite Clay as a Natural Remedy: a brief review, Iranian journal of public health, 46 (2017) 1176.
[22] S. Gu, X. Kang, L. Wang, E. Lichtfouse, C. Wang, Clay mineral adsorbents for heavy metal removal from wastewater: a review, Environmental Chemistry Letters, 17 (2019) 629-654.
[23] A.F.F. Farias, K.F. Moura, J.K. Souza, R.O. Lima, J.D. Nascimento, A.A. Cutrim, E. Longo, A.S. Araujo, J.R. Carvalho-Filho, A.G. Souza, Biodiesel obtained by ethylic transesterification using CuO, ZnO and CeO2 supported on bentonite, Fuel, 160 (2015) 357-365.
[24] V. Meille, Review on methods to deposit catalysts on structured surfaces, Applied Catalysis A: General, 315 (2006) 1-17.
[25] Z. Orolínová, A. Mockovčiaková, Structural study of bentonite/iron oxide composites, Materials Chemistry and Physics, 114 (2009) 956-961.
[26] A. Kaya, A.H. Ören, Adsorption of zinc from aqueous solutions to bentonite, Journal of Hazardous Materials, 125 (2005) 183-189.

[27] Z. Mirjafary, H. Saeidian, A. Sadeghi, F.M. Moghaddam, ZnO nanoparticles: An efficient nanocatalyst for the synthesis of β-acetamido ketones/esters via a multi-component reaction, Catalysis Communications, 9 (2008) 299-306.
[28] A. Hassanpour, R.H. Khanmiri, J. Abolhasani, ZnO nanoparticles as an efficient, heterogeneous, reusable, and ecofriendly catalyst for one-pot, three-component synthesis of 3, 4-dihydropyrimidin-2 (1 H)-(thio) one derivatives in water, Synthetic Communications, 45 (2015) 727-733.
[29] R. Tayebee, F. Javadi, G. Argi, Easy single-step preparation of ZnO nano-particles by sedimentation method and studying their catalytic performance in the synthesis of 2-aminothiophenes via Gewald reaction, Journal of Molecular Catalysis A: Chemical, 368 (2013) 16-23.
[30] G. Yuvaraja, C. Prasad, Y. Vijaya, M.V. Subbaiah, Application of ZnO nanorods as an adsorbent material for the removal of As (III) from aqueous solution: kinetics, isotherms and thermodynamic studies, International Journal of Industrial Chemistry, 9 (2018) 17-25.
[31] K. Nalwa, A. Thakur, N. Sharma, Synthesis of ZnO nanoparticles and its application in adsorption, Advanced Materials, 2 (2017) 697-703.
[32] M.N. Zafar, Q. Dar, F. Nawaz, M.N. Zafar, M. Iqbal, M.F. Nazar, Effective adsorptive removal of azo dyes over spherical ZnO nanoparticles, Journal of Materials Research and Technology, 8 (2019) 713-725.
[33] G. Feng, J. Ma, X. Zhang, Q. Zhang, Y. Xiao, Q. Ma, S. Wang, Magnetic natural composite Fe3O4-chitosan@bentonite for removal of heavy metals from acid mine drainage, Journal of Colloid and Interface Science, 538 (2019) 132-141.
[34] R. Mudzielwana, M.W. Gitari, S.A. Akinyemi, T.A.M. Msagati, Performance of Mn2+ modified Bentonite Clay for the Removal of Fluoride from Aqueous Solution, South African Journal of Chemistry, 71 (2018) 15-23.
[35] A. Ahmadi, R. Foroutan, H. Esmaeili, S. Tamjidi, The role of bentonite clay and bentonite clay@MnFe2O4 composite and their physico-chemical properties on the removal of Cr(III) and Cr(VI) from aqueous media, Environmental Science and Pollution Research, 27 (2020) 14044-14057.
[36] E. Rostami, R. Norouzbeigi, A. Rahbar, Thermal and chemical modification of bentonite for adsorption of an anionic dye, Advances in Environmental Technology, 4 (2018) 1-12.
[37] A. Aichour, H. Zaghouane-Boudiaf, Synthesis and characterization of hybrid activated bentonite/alginate composite to improve its effective elimination of dyes stuff from wastewater, Applied Water Science, 10 (2020) 146.
[38] M. Mahmood, S. Ismail, Fabrication and optimization of immobilized bentonite and TiO2 photocatalyst in unilayer and bilayer system for the photocatalytic adsorptive removal of methylene blue dye under UV light, AIP Conference Proceedings, AIP Publishing LLC, 2019, pp. 020039.
[39] F. Javadi, R. Tayebee, Preparation and characterization of ZnO/nanoclinoptilolite as a new nanocomposite and studying its catalytic performance in the synthesis of 2-aminothiophenes via Gewald reaction, Microporous and Mesoporous Materials, 231 (2016) 100-109.
[40] T. Wang, P. Zhao, N. Lu, H. Chen, C. Zhang, X. Hou, Facile fabrication of Fe3O4/MIL-101 (Cr) for effective removal of acid red 1 and orange G from aqueous solution, Chemical Engineering Journal, 295 (2016) 403-413.
[41] M. Bahrami, A. Nezamzadeh-Ejhieh, Effect of the supported ZnO on clinoptilolite nano-particles in the photodecolorization of semi-real sample bromothymol blue aqueous solution, Materials Science in Semiconductor Processing, 30 (2015) 275-284.
[42] S. Sohrabnezhad, A. Seifi, The green synthesis of Ag/ZnO in montmorillonite with enhanced photocatalytic activity, Applied Surface Science, 386 (2016) 33-40.
[43] I. Fatimah, S. Wang, D. Wulandari, ZnO/montmorillonite for photocatalytic and photochemical degradation of methylene blue, Applied Clay Science, 53 (2011) 553-560.
[44] T. Tatarchuk, M. Myslin, I. Mironyuk, M. Bououdina, A.T. Pędziwiatr, R. Gargula, B.F. Bogacz, P. Kurzydło, Synthesis, morphology, crystallite size and adsorption properties of nanostructured Mg–Zn ferrites with enhanced porous structure, Journal of Alloys and Compounds, 819 (2020) 152945.
[45] R.M. Kakhki, A. Karimian, H. Hasan-nejad, F. Ahsani, Zinc oxide–nanoclinoptilolite as a superior catalyst for visible photo-oxidation of dyes and green synthesis of pyrazole derivatives, Journal of Inorganic and Organometallic Polymers and Materials, 29 (2019) 1358-1367.

[46] S. Aslam, J. Zeng, F. Subhan, M. Li, F. Lyu, Y. Li, Z. Yan, In situ one-step synthesis of Fe3O4@ MIL-100 (Fe) core-shells for adsorption of methylene blue from water, Journal of colloid and interface science, 505 (2017) 186-195.
[47] I.D. Mall, V.C. Srivastava, N.K. Agarwal, Removal of Orange-G and Methyl Violet dyes by adsorption onto bagasse fly ash—kinetic study and equilibrium isotherm analyses, Dyes and pigments, 69 (2006) 210-223.
[48] M. Ishaq, K. Saeed, I. Ahmad, S. Sultan, S. Akhtar, Coal ash as a low cost adsorbent for the removal of xylenol orange from aqueous solution, Iranian Journal of Chemistry and Chemical Engineering (IJCCE), 33 (2014) 53-58.
[49] I. Mall, V. Srivastava, G. Kumar, I. Mishra, Characterization and utilization of mesoporous fertilizer plant waste carbon for adsorptive removal of dyes from aqueous solution, Colloids and Surfaces A: Physicochemical and Engineering Aspects, 278 (2006) 175-187.
[50] M.A.M. Salleh, D.K. Mahmoud, W.A.W.A. Karim, A. Idris, Cationic and anionic dye adsorption by agricultural solid wastes: A comprehensive review, Desalination, 280 (2011) 1-13.
[51] S. Dawood, T. Sen, Review on dye removal from its aqueous solution into alternative cost effective and non-conventional adsorbents, Journal of Chemical and Process Engineering, 1 (2014) 1-11.
[52] A.-H. Rasmey, A.A. Aboseidah, A.K. Youssef, Application of Langmuir and Freundlich Isotherm Models on Biosorption of Pb^{2+} by Freez-dried Biomass of Pseudomonas aeruginosa, Egyptian Journal of Microbiology, 53 (2018) 37-48.
[53] N. Benderdouche, B. Bestani, M. Hamzaoui, The use of linear and nonlinear methods for adsorption isotherm optimization of basic green 4-dye onto sawdust-based activated carbon, J. Mater. Environ. Sci, 9 (2018) 1110-1118.
[54] F. Zhang, W. Song, J. Lan, Effective removal of methyl blue by fine-structured strontium and barium phosphate nanorods, Applied Surface Science, 326 (2015) 195-203.
[55] A. Jarrah, S. Farhadi, Encapsulation of $K_6P_2W_{18}O_{62}$ into magnetic nanoporous Fe_3O_4/MIL-101 (Fe) for highly enhanced removal of organic dyes, Journal of Solid State Chemistry, 285 (2020) 121264.
[56] Z. Ding, W. Wang, Y. Zhang, F. Li, J.P. Liu, Synthesis, characterization and adsorption capability for Congo red of CoFe2O4 ferrite nanoparticles, Journal of Alloys and Compounds, 640 (2015) 362-370.
[57] S. Aslam, J. Zeng, F. Subhan, M. Li, F. Lyu, Y. Li, Z. Yan, In situ one-step synthesis of Fe3O4@MIL-100(Fe) core-shells for adsorption of methylene blue from water, Journal of Colloid and Interface Science, 505 (2017) 186-195.
[58] X. Liu, W. Gong, J. Luo, C. Zou, Y. Yang, S. Yang, Selective adsorption of cationic dyes from aqueous solution by polyoxometalate-based metal–organic framework composite, Applied Surface Science, 362 (2016) 517-524.
[59] H. Liu, X. Ren, L. Chen, Synthesis and characterization of magnetic metal–organic framework for the adsorptive removal of Rhodamine B from aqueous solution, Journal of industrial and engineering chemistry, 34 (2016) 278-285.
[60] M.A. Al-Kazragi, D.T. Al-Heetimi, O.S. Al-Khazrajy, Xylenol orange removal from aqueous solution by natural bauxite (BXT) and BXT-HDTMA: kinetic, thermodynamic and isotherm modeling, Desalination and Water Treatment, 145 (2019) 369-377.
[61] S. Wang, D. Yu, Y. Huang, J. Guo, The adsorption of sulphonated azo-dyes methyl orange and xylenol orange by coagulation on hollow chitosan microsphere, Journal of Applied Polymer Science, 119 (2011) 2065-2071.
[62] M. Zhu, G. Diao, Synthesis of porous Fe3O4 nanospheres and its application for the catalytic degradation of xylenol orange, The Journal of Physical Chemistry C, 115 (2011) 18923-18934.
[63] C.F.L.L.Z. Zhu, Treatment of Xylenol Orangeand Methylene Blue with Fresh MnO_2, dvances in Fine Petrochemicals, (2007) 15.